
ICNN-enhanced 2SP: Leveraging input convex neural networks for solving two-stage stochastic programming

Yu Liu Fabricio Oliveira*

Department of Mathematics and Systems Analysis, Aalto University, Espoo, Finland

Abstract

Two-stage stochastic programming (2SP) offers a basic framework for modelling decision-making under uncertainty, yet scalability remains a challenge due to the computational complexity of recourse function evaluation. Existing learning-based methods like Neural Two-Stage Stochastic Programming (Neur2SP) employ neural networks (NNs) as recourse function surrogates but rely on computationally intensive mixed-integer programming (MIP) formulations. We propose ICNN-enhanced 2SP, a method that leverages Input Convex Neural Networks (ICNNs) to exploit linear programming (LP) representability in convex 2SP problems. By architecturally enforcing convexity and enabling exact inference through LP, our approach eliminates the need for integer variables inherent to the conventional MIP-based formulation while retaining an exact embedding of the ICNN surrogate within the 2SP framework. This results in a more computationally efficient alternative that maintains solution quality. Comprehensive experiments reveal that ICNNs incur only marginally longer training times while achieving validation accuracy on par with their MIP-based counterparts. Across benchmark problems, ICNN-enhanced 2SP often exhibits considerably faster solution times than the MIP-based formulations while preserving solution quality, with these advantages becoming significantly more pronounced as problem scale increases. For the most challenging instances, the method achieves speedups of up to $100\times$ and solution quality superior to MIP-based formulations.

1 Introduction

Two-stage stochastic programming (2SP) is a cornerstone modelling framework for decision-making under uncertainty, enabling optimal resource allocation in the face of unpredictable future events. In this, initial (first-stage) decisions are made before uncertainty is resolved, followed by adjustment (recourse, or second-stage) decisions once the random variables have unfolded. Industries such as power (Römisch and Vigerske, 2010) and petrochemical sectors (Khor et al., 2008) rely on 2SP to incorporate uncertainty in their optimisation modelling, utilising it as a standard tool in planning activities.

Sample Average Approximation (SAA) (Shapiro and Homem-de Mello, 1998) is a foundational technique for 2SP, in which the expected value of the second-stage problem is replaced with a finite-scenario approximation. Though computationally tractable, SAA faces a fundamental trade-off: insufficient scenarios may fail to accurately represent the random phenomena, while larger samples increase computational demands. To alleviate this limitation, scenario reduction techniques (Heitsch and Römisch, 2003) are often applied, but these risk omitting critical scenarios, undermining solution robustness. These shortcomings have prompted the adoption of specialised decomposition approaches,

*Corresponding author: fabricio.oliveira@aalto.fi.

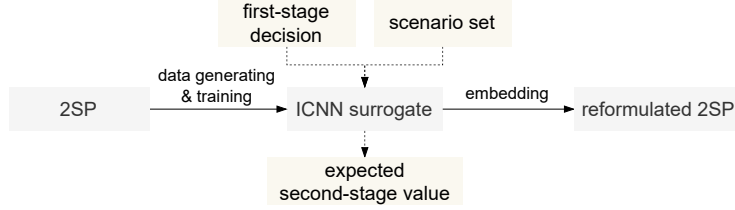


Figure 1: Overview of the proposed optimisation methodology.

including Benders-based (Sherali and Fraticelli, 2002) and Lagrangian decomposition-based methods (Carøe and Schultz, 1999), which decompose the problem into smaller, more manageable subproblems. By exploiting problem structure (e.g., separability and duality), these methods mitigate SAA’s scalability challenges and reduce dependency on scenario sampling (Küçükyavuz and Sen, 2017). However, their efficacy remains contingent on problem-specific properties, such as linearity or convexity, and often requires meticulous algorithmic tuning. Despite developments in decomposition methods (Varga et al., 2024), these limitations persist, driving exploration of alternative approaches that leverage machine learning (ML).

Recent advances in learning-based methods for 2SP have explored surrogate models to approximate complex value functions. Dai et al. (2021) proposed a neural network (NN) to map problem instances to piecewise-linear value functions within low-dimensional latent spaces. Larsen et al. (2024) replace later-stage Benders subproblems with ML predictions to accelerate decomposition. Yilmaz and Büyüktaktakın (2024) decompose 2SP into multi-agent structures trained on sampled scenarios. While these approaches demonstrate the advantages of surrogate modelling, they are relatively less generalisable, constrained by specific problem components or reliance on bespoke architectures. In contrast, Neur2SP (Neural Two-Stage Stochastic Programming) (Dumouchelle et al., 2022) presents a general framework by employing NNs to approximate the expected recourse function, motivated by the embedding of a trained NN surrogate (Fischetti and Jo, 2018). However, Neur2SP’s generality comes at a cost: embedding NNs with rectified linear unit (ReLU) activations into optimisation models requires mixed-integer programming (MIP) formulations that scale with the network size, leading to computational intractability for deeper or wider architectures. This tension between generality and efficiency underscores the need for architectures that balance expressivity with tractability.

Input Convex Neural Networks (ICNNs) (Amos et al., 2017) have emerged as a promising alternative for surrogate modelling due to their ability to fit general convex functions while retaining the flexibility and expressivity of NNs. Unlike typical feed-forward networks, ICNNs are architecturally constrained to ensure convexity with respect to their inputs, enabling exact inference through linear programming (LP) formulations (Duchesne et al., 2021). This property renders them particularly advantageous for embedding within large-scale optimisation frameworks. Although ICNNs cannot model non-convex recourse functions, a limitation compared to ReLU NNs, many real-world 2SP problems in inventory management, energy dispatch, and portfolio optimisation inherently exhibit convex structure (Agrawal and Jia, 2019; Zhong et al., 2021; Luxenberg and Boyd, 2024). Despite their promise, prior research has predominantly focused on applying ICNNs for function approximation and system modelling, such as learning Optimal Power Flow (OPF) value functions (Chen et al., 2020; Rosemberg et al., 2024) or representing system dynamics in optimal control (Yang and Bequette, 2021; Bünning et al., 2021; Jiang et al., 2022; Wang et al., 2024; Omid et al., 2024). However, their potential in surrogate-based optimisation, specifically for approximating convex recourse functions in 2SP, remains underexplored. As such, our work bridges this gap by unlocking efficient and scalable solutions for 2SP, leveraging the inherent convexity and computational tractability of LP.

In particular, we present several interconnected contributions within a surrogate-based optimisation framework by integrating ICNNs into the 2SP paradigm, as we illustrate in Figure 1. First, we exploit the LP representability of ICNNs to eliminate integer variables inherent to conventional MIP-based embeddings. Second, we propose the first integration of ICNNs in 2SP, training them to approximate the expected value function while preserving convexity. Third, extensive numerical experiments show that our method achieves solution quality comparable to Neur2SP (Dumouchelle et al., 2022) while reducing computational time, especially for large-scale instances, enabling application to time-critical decision problems.

The paper proceeds as follows: Section 2 reviews 2SP and ICNN fundamentals; Section 3 analyses the convexity of the surrogate target; Section 4 details the process of ICNN surrogate training and embeddings; Section 5 presents the numerical experiments involving three different 2SP problems; Section 6 concludes with key findings and opening research directions.

2 Preliminaries

2.1 Two-stage stochastic programming

Let $x \in \mathbb{R}^n$ denote first-stage decisions, $y \in \mathbb{R}^{n_y}$ the recourse (second-stage) decisions, and ξ the relevant random variable. The stochastic components of the second-stage data $q(\xi) \in \mathbb{R}^{n_y}$, $W(\xi) \in \mathbb{R}^{m_y \times n_y}$, $h(\xi) \in \mathbb{R}^{m_y}$ and $T(\xi) \in \mathbb{R}^{m_y \times n}$ are determined by the realisation of ξ . The general linear 2SP formulation is

$$\min_x c^\top x + \mathcal{Q}(x) \quad (1a)$$

$$\text{s.t. } Ax = b, \quad (1b)$$

$$x \geq 0, \quad (1c)$$

where $A \in \mathbb{R}^{m \times n}$, $b \in \mathbb{R}^m$, $c \in \mathbb{R}^n$, $\mathcal{Q}(x) = \mathbb{E}_\xi[Q(x, \xi)]$ and the second-stage problem is

$$Q(x, \xi) = \min_y \{q(\xi)^\top y \mid W(\xi)y = h(\xi) - T(\xi)x, y \geq 0\}, \quad (2)$$

which evaluates to the optimal second-stage cost under realisation ξ given the first-stage decision x . We assume relatively complete recourse, ensuring Q is feasible for any x satisfying (1b) and (1c).

The decision process follows $x \rightarrow \xi \rightarrow y(x, \xi)$, where y is chosen to minimise $Q(x, \xi)$. We assume ξ has a known probability distribution with support Ξ . In practical implementations, Ξ is treated as a discrete and finite set where each realisation $\xi_s \in \Xi$ for $s \in S \equiv \{1, \dots, |\Xi|\}$ represents a scenario. This yields the deterministic equivalent formulation with a finite number of variables and constraints:

$$\min_x c^\top x + \sum_{s \in S} p_s q_s^\top y_s \quad (3a)$$

$$\text{s.t. } Ax = b, \quad x \geq 0 \quad (3b)$$

$$T_s x + W_s y_s = h_s, \quad \forall s \in S \quad (3c)$$

$$y_s \geq 0, \quad \forall s \in S, \quad (3d)$$

where p_s is the probability associated with scenario s . This so-called *extensive form* (EF) (3) provides a tractable formulation. However, it suffers from scalability issues as both the number of variables and constraints increase linearly with the cardinality of the scenario set $|\Xi|$. As such, for variants involving mixed-integer decision variables, the computational demand increases substantially for larger scenario sets.

2.2 ICNN architectures

We consider a fully connected K -layer ICNN, as illustrated in Figure 2, to construct a scalar-valued NN $\hat{f}(z_0; \theta)$ that approximates a target function f . Here, z_0 denotes input vectors and θ represents network parameters. The activation for each layer can be expressed as:

$$z_{k+1} = \sigma(W_k z_k + S_k z_0 + b_k), \quad k = 0, \dots, K-1, \quad (4)$$

where z_k for $k \geq 1$ is obtained by applying an activation function $\sigma(\cdot)$, with initial conditions $W_0 \equiv 0$. The output of the network is $\hat{f}(z_0; \theta) = z_K$ with $\theta = \{W_{1:K-1}, S_{0:K-1}, b_{0:K-1}\}$.

The surrogate function \hat{f} is guaranteed to be convex in z_0 provided that $W_{1:K-1}$ are non-negative and the activation function $\sigma(\cdot)$ (ReLU in our case) is convex and non-decreasing (Amos et al., 2017). This follows standard results relating to convexity-preserving operations applied to convex functions: (i) non-negative sums of convex functions are convex; (ii) the composition of a convex function with a convex non-decreasing function retains convexity. Another relevant feature of ICNNs is the presence *skip connections* parameterised by S_k , which directly propagates the input z_0 to deeper layers. This design aims to mitigate the restrictive effects of the non-negativity constraints imposed on W_k . Notably, these skip connections preserve convexity as the sum of a convex function (from previous layers) and a linear function (from the skip connections) remains convex.

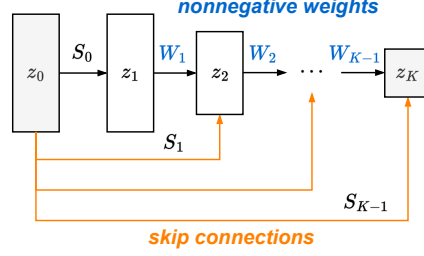


Figure 2: Architecture of a fully connected ICNN.

2.3 Exact inference in ICNNs

Unlike conventional NNs, which generate predictions solely through feedforward propagation of inputs across layers, the original formulation of ICNNs requires the solution of an optimisation problem as a subroutine to derive predictions. For a fully connected ICNN as described in (4), inference for a given input z_0 is mathematically equivalent to solving the following LP problem (Amos et al., 2017):

$$\min_{z_k} z_K \quad (5a)$$

$$\text{s.t. } z_{k+1} \geq W_k z_k + S_k z_0 + b_k, \quad k = 0, \dots, K-1 \quad (5b)$$

$$z_k \geq 0, \quad k = 1, \dots, K-1. \quad (5c)$$

In this formulation, the non-linearity of ReLU activations and layer-wise equality constraints are transformed into inequalities via an *epigraph* representation, exploiting the fact that ReLU is a piecewise-linear function. One may note that the minimisation objective enforces that at least one constraint in (5b) or (5c) becomes active at the optimal solution, recovering the original network's feedforward behaviour. This transformation provides a principled framework for embedding a trained ICNN surrogate into larger optimisation problems, as it offers not only an exact representation of the NN but also preserves computational tractability inherent to LP.

3 Convexity analysis

This section establishes the theoretical foundation for using ICNNs as surrogates for the second-stage cost $Q(x)$ in 2SP. Since ICNNs inherently preserve convexity, their effectiveness hinges on whether $Q(x)$ is convex. As $Q(x)$ is evaluated by solving the second-stage problem $Q(x, \xi)$ for each scenario, it becomes a convex function of x only if the second-stage problem itself is convex. A convex problem can take two equivalent forms: minimising a convex function or maximising a concave function - as these are mathematically equivalent through the negation of the objective - over a convex feasible region. We analyse three variants of 2SP problems to demonstrate that $Q(x)$ retains its convexity under broad conditions, even when discrete variables are present in the second-stage problem.

Case 1: continuous first- and second-stage variables. When $x \in \mathbb{R}_+^n$ and $y_s \in \mathbb{R}_+^{n_y}, \forall s \in S$, the second-stage problem $Q(x, \xi_s)$ is an LP. By LP duality, we have that

$$Q(x, \xi_s) = \max_{\pi} \{ \pi^\top (h_s - T_s x) \mid W_s^\top \pi \leq q_s \}, \quad (6)$$

where π represents the dual variable associated with the equality constraint $W_s y = h_s - T_s x$. The dual objective is affine in x and the dual feasible set

$$D_s(x) = \{ \pi \in \mathbb{R}^{m_y} \mid W_s^\top \pi \leq q_s \}$$

constitutes a convex polyhedron. By the fundamental theorem of LP, the maximum of the dual objective is attained at an extreme point (vertex) of $D_s(x)$, given that the relatively complete recourse assumption guarantees that (6) is feasible and bounded. Let $\pi_1, \pi_2, \dots, \pi_K$ denote the finite set of extreme points of $D_s(x)$. Thus:

$$Q(x, \xi_s) = \max_{k \in \{1, \dots, K\}} \{ -\pi_k^\top T_s x + \pi_k^\top h_s \}. \quad (7)$$

Each term $-\pi_k^\top T_s x + \pi_k^\top h_s$ is affine in x , so $Q(x, \xi_s)$ is the pointwise maximum of affine functions. As affine functions are convex and the pointwise maximum preserves convexity (Boyd and Vandenberghe,

2004, Section 3.2.3), $Q(x, \xi_s)$ is convex in x . The expected second-stage cost $\mathbb{E}_\xi[Q(x, \xi)] = \sum_{s \in S} p_s Q(x, \xi_s)$ is a convex combination of convex functions $Q(x, \xi_s)$, since $0 \leq p_s \leq 1, \forall s \in S$, and $\sum_{s \in S} p_s = 1$. Thus, $Q(x)$ is convex in x .

Case 2: mixed-integer first- and continuous second-stage variables. Consider $x \in \mathcal{X}$ where $\mathcal{X} = \{x \in \mathbb{Z}_+^n \mid Ax = b\}$ and $y_s \in \mathbb{R}_+^{n_y}$. Let us define $\mathcal{X}_{\text{relax}} = \{x \in \mathbb{R}_+^n \mid Ax = b\}$ as the continuous relaxation of \mathcal{X} , and $\text{conv}(\mathcal{X})$ as the convex hull of \mathcal{X} . From Case 1, we established that $Q(x)$ is convex over $\mathcal{X}_{\text{relax}}$. Since $\text{conv}(\mathcal{X}) \subset \mathcal{X}_{\text{relax}}$, the function $Q(x)$ is also convex over $\text{conv}(\mathcal{X})$. Thus, there must be λ values with $\lambda \in [0, 1]$ for which all points in \mathcal{X} can be represented as $x_\lambda = \lambda x_1 + (1 - \lambda)x_2$ for $x_1, x_2 \in \text{conv}(\mathcal{X})$. As we have established that $Q(x)$ is convex over $\text{conv}(\mathcal{X})$, the convexity property $Q(x_\lambda) \leq \lambda Q(x_1) + (1 - \lambda)Q(x_2)$ must hold for these points x_λ and their respective λ values. Thus, as x_λ collectively form \mathcal{X} , $Q(x)$ is convex over \mathcal{X} , though not continuous due to the discrete nature of \mathcal{X} . We highlight that, when x is mixed-integer, the convexity of $Q(x)$ trivially applies by the same reasoning.

Case 3: mixed-integer first- and second-stage variables. Following Case 2, we first demonstrate that $Q(x, \xi_s)$ remains convex in x when $y_s \in \mathbb{Z}_+^{n_y}$. For a fixed $x \in \mathcal{X}$, we define the feasible region of the second-stage problem as:

$$F_s(x) = \{y_s \in \mathbb{Z}_+^{n_y} \mid W_s y_s = h_s - T_s x\}. \quad (8)$$

Let $\text{conv}(F_s(x))$ be the convex hull of this set. Since the optima lie at extreme points of the feasible set in LP; and the extreme points of $\text{conv}(F_s(x))$ are precisely the integer points in $F_s(x)$, we have:

$$Q(x, \xi_s) = \min_{y_s \in F_s(x)} q_s^\top y_s = \min_{y_s \in \text{conv}(F_s(x))} q_s^\top y_s. \quad (9)$$

With this equivalence shown, we can apply LP duality as in Case 1. Following the same reasoning from Case 1, we conclude $Q(x, \xi_s)$ is the pointwise maximum of affine functions in x , and thus convex. Consequently, $Q(x) = \sum_{s \in S} p_s Q(x, \xi_s)$ remains convex in x . For mixed-integer second-stage variables, the resulting problem combines the structures analysed in Cases 1 and the integer second-stage variables case. Thus, our convexity analysis extends naturally to mixed-integer recourse.

Remark. *The convexity of $Q(x)$ extends to second-stage problems with nonlinear convex constraints, provided that appropriate constraint qualification (CQ) conditions are satisfied, such as Slater's CQ condition (Boyd and Vandenberghe, 2004, Section 5.2.3), since strong duality still applies under CQ. In this more general setting, the dual formulation transforms $Q(x, \xi_s)$ into the pointwise maximum of convex functions in x . Following similar reasoning as in Case 1, $Q(x)$ preserves its convexity. Furthermore, if the first-stage problem includes a nonlinear convex objective, along with nonlinear convex inequality constraints and affine equality constraints, the recourse function remains convex in x (Birge and Louveaux, 2011, Section 3.5).*

In summary, for a broad class of 2SP problems, the recourse function $Q(x)$ inherits a piecewise convex structure, even accommodating relatively challenging instances with strategic integer decisions in the first stage and operational adjustments (continuous) or logical switches (binary) in recourse actions. Such structural regularity makes approximation via ICNNs advantageous, as they inherently preserve convexity while learning surrogate models of $Q(x)$, enabling the embedding of the ICNN surrogates into the original 2SP for efficient solving.

4 Methodology

This section presents our ICNN-enhanced framework for 2SP that directly leverages the convexity properties of $Q(x)$. By exploiting this inherent convexity, we employ ICNNs as recourse function approximators and embed this surrogate into the first-stage problem to obtain a reformulated 2SP without introducing integer variables.

4.1 Base architecture

Building on the extensive form (3), Neur2SP constructs a surrogate model $\hat{Q}(x)$ to explicitly model the expected second-stage cost $Q(x)$ through two sequential transformations:

(i) *Scenario Encoding*: consists of the x -independent processing of each scenario ξ_s through a shared network Ψ^1 to transform each scenario into a latent feature vector, followed by mean-aggregation

and final encoding via another network Ψ^2 :

$$\xi_\lambda = \Psi^2 \left(\frac{1}{|S|} \sum_{s=1}^{|S|} \Psi^1(\xi_s) \right), \quad (10)$$

where ξ_λ serves as a compact representation of the entire scenario ensemble while preserving its statistical features.

(ii) *Decision Mapping*: represents a conventional ReLU NN Φ that combines first-stage decisions x with scenario encoding ξ_λ to predict $\mathbb{E}_\xi[Q(x, \xi)]$:

$$\hat{Q}(x) = \Phi(x, \xi_\lambda), \quad (11)$$

without requiring separate evaluations for each scenario.

While effective for general 2SP, this architecture becomes suboptimal for convex problems due to its MIP-based surrogate embeddings. The embedding of ReLU NNs as MIP constraints within optimisation problems is detailed in Appendix A. In our approach, we retain Neur2SP’s core architecture for scenario processing while being specialised for convex 2SP models. The key difference lies in Φ ’s architecture: Φ is formulated as an ICNN since $Q(x, \xi_s)$ is convex in x (per Section 3).

4.2 Surrogate modelling

For convex 2SP problems, we define Φ as:

$$\Phi_{\text{ICNN}}(x, \xi_\lambda) = z_K, \quad (12)$$

where layer activations z_k follow:

$$z_{k+1} = \sigma(W_k z_k + S_k[x, \xi_\lambda] + b_k), \quad k = 0, \dots, K-1, \quad (13)$$

with $z_0 = [x, \xi_\lambda]$, $W_0 \equiv 0$ and architectural constraints: (i) $W_k \geq 0$; and (ii) $\sigma(\cdot)$ is convex and non-decreasing. This ensures Φ_{ICNN} is convex in x , matching the convexity of $Q(x)$ while preserving Neur2SP’s ability to process arbitrary scenario sets through the encoder (Ψ_1 and Ψ_2).

In essence, the ICNN surrogate learns to map (x, ξ_λ) pairs to $Q(x)$ values, with ξ_λ acting as a “context vector” that encapsulates the probability distribution formed by the scenario set S . As such, it enables the ICNN to learn a family of convex functions in x , with each specific realisation of ξ_λ generating a distinct convex function that models $Q(x)$ for its corresponding scenario distribution.

The training process follows a supervised paradigm: (i) generate training pairs $(x^{(i)}, \mathbb{E}_\xi[Q(x^{(i)}, \xi)])$ by solving EF instances, where i indexes the training example; (ii) train Ψ_1 , Ψ_2 and Φ_{ICNN} jointly to minimise the mean squared error (MSE):

$$\min_{\Theta} \sum_i \left(\Phi_{\text{ICNN}} \left(x^{(i)}, \Psi^2 \left(\frac{1}{|S|} \sum_{s=1}^{|S|} \Psi^1(\xi_s^{(i)}) \right) \right) - \mathbb{E}_\xi[Q(x^{(i)}, \xi)] \right)^2, \quad (14)$$

where $\Theta = \{W_k, S_k, b_k\} \cup \{\Psi^1, \Psi^2\}$ represents the complete set of trainable parameters. Importantly, once trained, the model generalises to arbitrary second-stage scenario sets without requiring retraining, eliminating scenario set-specific training overhead.

4.3 Surrogate embedding

The ICNN architecture enables an exact convex optimisation formulation to be used instead of Neur2SP’s MIP formulation. Building on the exact inference equivalence (Section 2.3), we reformulate the 2SP as:

$$\min_x \quad c^\top x + z_K \quad (15a)$$

$$\text{s.t.} \quad z_{k+1} \geq W_k z_k + S_k[x, \xi_\lambda] + b_k, \quad k = 0, \dots, K-1 \quad (15b)$$

$$z_k \geq 0, \quad k = 1, \dots, K \quad (15c)$$

$$x \in \mathcal{X}. \quad (15d)$$

At deployment, ξ_λ is precomputed offline from a given scenario set, ensuring the problem remains convex in x .

This alternative embedding incurs important methodological advantages. Compared to a MIP-based formulation, our approach significantly reduces the mathematical programming formulation scale and computational complexity. The conventional ReLU encoding necessitates introducing N binary variables, N continuous slack variables, and N activation value variables (where N is the neuron count). These auxiliary binary variables introduce combinatorial complexity that scales exponentially with network depth and width. In contrast, by leveraging ICNN’s architectural properties, our formulation eliminates both these auxiliary integer variables and continuous slack variables entirely, yielding a more compact representation, which in turn benefits computational efficiency.

5 Experiments

In this section, we report the results of our proposed ICNN-enhanced method across the three problem settings from the aspects of training and solving performance.

5.1 Experimental setup

All experiments were conducted on a Triton computing cluster maintained by the Aalto Science-IT project, utilising an Intel Xeon Gold 6148 CPU and an NVIDIA Tesla H100 GPU with 64 GB of RAM. Our code extends Neur2SP’s codebase (Patel and Dumouchelle, 2022) by augmenting it to include all necessary ICNN-related functionalities. The implementation uses Python 3.11.5 with Gurobi 11.0.2 (Gurobi Optimization, LLC, 2024) as the optimisation solver, PyTorch 2.0.1 (Paszke et al., 2019) and scikit-learn 1.3.0 (Pedregosa et al., 2011) for NN training. Full reproducibility materials are provided at <https://github.com/Lycle/ICNN2SP>.

We evaluate our method on three canonical 2SP problems which are also taken as benchmark problems in Neur2SP (Dumouchelle et al., 2022): the capacitated facility location problem (CFLP) (Cornuejols et al., 1991), the stochastic server location problem (SSLP) (Ntaimo and Sen, 2005), and the investment problem (INVP) (Schultz et al., 1998). Problem instances are denoted by type followed by structural parameters, with the final parameter indicating scenario count. Detailed descriptions are provided in Appendix B. The EF serves as the ground-truth baseline (considering a 3-hour time limit). We compare both ICNN-enhanced 2SP and Neur2SP against EF to contextualise performance.

To ensure direct comparability with Neur2SP, we replicate their instance generation protocol, including uncertainty distributions and scenario sampling methods. We generate 5,000 first-stage solutions by uniformly sampling the feasible region. For each solution, the expected recourse cost is approximated by solving its second-stage problem for a random subset of scenarios, with the number of scenarios per solution randomly selected up to 100, which balances computational efficiency with the diversity of scenarios. Further details on data generation are provided in Appendix C. For both methods, we conduct a random search over 100 hyperparameter configurations for NN architecture selection, detailed in Appendix D. To mitigate solver-induced variability, Gurobi’s parameters are fixed across all runs, as detailed in Appendix E.

5.2 Results and discussion

Tables 1 to 4 report our experimental results. In addition, we include supplementary results with the objective values in Appendix F and results for the SSLP instances from the Stochastic Integer Programming Test Problem Library (SIPLIB) (Ahmed et al., 2015) in Appendix G. We also analyse the variable counts in Appendix H to compare formulation size.

Both methods share the same structural design for Scenario Encoding (Ψ^1 and Ψ^2) while differing in the architectural choice of Decision Mapping (Φ): our method uses ICNNs while Neur2SP employs conventional ReLU NNs, which constitutes the primary source of training performance differences. As shown in Table 1, both methods exhibit training times within the same order of magnitude, with ICNNs requiring only marginally longer training due to their convexity constraints. This modest overhead is counterbalanced by their comparable or superior validation accuracy, achieving lower mean absolute error (MAE) in 7 out of 10 problem instances. These results demonstrate that the convexity constraints do not significantly compromise the expressive power of the NN while presenting mathematical properties that enable more efficient downstream optimisation.

Table 1: Training times and MAE on validation when applying ICNN-enhanced 2SP (ICNN) and Neur2SP (NN). Samples split 80%-20% for train-validation, with the best model selected on validation within the given epochs.

Problem	Training time (s)		Validation MAE	
	ICNN	NN	ICNN	NN
CFLP_10_10	359.41	279.96	248.441	257.213
CFLP_25_25	288.77	275.49	313.604	341.477
CFLP_50_50	290.76	270.52	558.073	569.384
SSLP_5_25	295.31	270.52	16.862	16.594
SSLP_15_45	295.36	275.74	27.294	29.062
SSLP_10_50	292.08	273.90	17.372	14.105
INVP_B_E	312.51	283.28	2.050	2.179
INVP_B_H	312.04	285.02	1.902	2.031
INVP_I_E	362.10	336.93	2.480	2.465
INVP_I_H	312.27	284.45	2.159	2.245

Table 2: CFLP results (averaged over 11 instances per row; EF averages include only instances where EF found feasible solutions within 3h). Gap: relative objective difference (%) of ICNN-enhanced 2SP (ICNN-EF) and Neur2SP (NN-EF) compared to EF; negative values indicate better solutions for minimisation. Solving time: runtime (s); $\sim 10,800$ indicates time limit reached. **Bold** indicates better performance.

Problem	Gap (%)		Solving time (s)		
	ICNN-EF	NN-EF	ICNN	NN	EF
CFLP_10_10_100	0.57	0.51	0.29	0.39	8,491.85
CFLP_10_10_500	0.15	0.00	0.29	0.39	10,800.05
CFLP_10_10_1000	-0.02	-0.27	0.29	0.39	10,800.29
CFLP_25_25_100	2.19	3.37	0.39	10.31	10,800.05
CFLP_25_25_500	1.74	2.63	0.40	10.37	10,800.12
CFLP_25_25_1000	0.51	1.48	0.40	10.07	10,800.33
CFLP_50_50_100	3.36	18.17	0.81	84.07	10,800.63
CFLP_50_50_500	-9.82	3.06	0.84	84.32	10,800.16
CFLP_50_50_1000	-12.82	-0.28	0.84	84.39	10,800.29

Table 3: SSLP results (averaged over 12 instances per row). All settings and metric definitions follow Table 2.

Problem	Gap(%)		Solving time (s)		
	ICNN-EF	NN-EF	ICNN	NN	EF
SSLP_5_25_50	0.12	0.12	0.13	0.25	1.58
SSLP_5_25_100	0.02	0.02	0.12	0.25	5.18
SSLP_15_45_5	2.65	18.09	0.16	0.20	1.94
SSLP_15_45_10	2.57	18.38	0.18	0.20	32.74
SSLP_15_45_15	2.11	18.72	0.20	0.21	605.22
SSLP_10_50_50	0.00	0.00	0.27	0.76	9,007.88
SSLP_10_50_100	0.00	0.00	0.26	0.76	10,800.04
SSLP_10_50_500	0.00	0.00	0.28	0.77	10,800.21
SSLP_10_50_1000	-2.22	-2.22	0.28	0.77	10,803.79
SSLP_10_50_2000	-102.68	-102.68	0.29	0.78	10,800.14

Tables 2–4 reveal consistent performance advantages for ICNN-enhanced 2SP across problem classes. For CFLP, our method demonstrates superior scalability, achieving $1.3\times$ speedups for small instances and up to $100\times$ faster solving times for more complex problem class (CFLP_50_50) when compared to Neur2SP, while maintaining comparable or better solution quality. For SSLP, our approach achieves $2\times$ speedups with identical optimality gaps for SSLP_5_25, a substantial gap reduction with $1.1\text{--}1.2\times$ speedups for SSLP_15_45, and $3\times$ faster solution times with matching solution quality for SSLP_10_50 instances. For INVP, while absolute solving time differences are marginal (≤ 0.03 s), ICNN-enhanced 2SP consistently delivers superior solution quality across most instances, often with considerable optimality gap improvements over Neur2SP.

Overall, ICNN-enhanced 2SP demonstrates computational advantages across various problem settings, with solution quality matching or exceeding Neur2SP in 80% of cases. While training requires modest

Table 4: INVP results (one instance per row). All settings and metric definitions follow Table 2.

Problem	Gap (%)		Solving time (s)		
	ICNN-EF	NN-EF	ICNN	NN	EF
INVP_B_E_4	11.06	10.80	0.06	0.15	0.00
INVP_B_E_9	5.60	4.31	0.07	0.10	0.01
INVP_B_E_36	3.28	4.58	0.06	0.10	0.05
INVP_B_E_121	3.07	2.85	0.06	0.09	1.32
INVP_B_E_441	3.10	3.18	0.06	0.10	125.60
INVP_B_E_1681	0.98	0.21	0.07	0.10	10,800.00
INVP_B_E_10000	-1.59	-1.64	0.07	0.11	10,808.33
INVP_B_H_4	8.81	8.81	0.06	0.08	0.01
INVP_B_H_9	5.04	5.04	0.07	0.09	0.01
INVP_B_H_36	1.61	1.61	0.07	0.08	1.18
INVP_B_H_121	1.77	1.77	0.06	0.08	60.09
INVP_B_H_441	2.13	2.13	0.06	0.09	322.05
INVP_B_H_1681	0.69	0.69	0.06	0.09	10,800.01
INVP_B_H_10000	-2.72	-2.72	0.07	0.10	10,808.33
INVP_I_E_4	4.78	17.32	0.05	0.08	0.00
INVP_I_E_9	1.07	7.01	0.04	0.07	0.01
INVP_I_E_36	0.37	3.98	0.06	0.07	0.03
INVP_I_E_121	0.17	2.88	0.06	0.08	0.39
INVP_I_E_441	0.11	3.22	0.04	0.07	39.73
INVP_I_E_1681	0.42	3.39	0.05	0.07	10,800.00
INVP_I_E_10000	0.22	3.50	0.05	0.08	10,800.09
INVP_I_H_4	13.78	13.78	0.07	0.06	0.01
INVP_I_H_9	5.85	9.12	0.05	0.07	0.01
INVP_I_H_36	3.69	4.97	0.06	0.07	0.40
INVP_I_H_121	3.75	4.01	0.05	0.07	7.27
INVP_I_H_441	1.27	3.15	0.05	0.07	10,800.00
INVP_I_H_1681	-0.41	-0.34	0.05	0.07	10,800.01
INVP_I_H_10000	0.27	0.25	0.06	0.08	10,800.03

overhead (10% longer on average), this upfront investment enables acceleration during optimisation through LP-driven formulation.

6 Conclusions

This work establishes ICNNs as an alternative framework for solving convex 2SP, offering an effective pathway to reconcile computational efficiency with solution quality. Our framework, ICNN-enhanced 2SP, integrates ICNNs as surrogates for the expected recourse function, showing that its architectural convexity constraints can be strategically harnessed rather than being limitations. Across diverse problem classes, ICNN-enhanced 2SP outperforms existing MIP-based methodologies, with its computational advantages becoming more pronounced as problem scale increases. The computational efficiency makes our approach viable for time-critical decision-making applications requiring frequent resolving, such as real-time power dispatch and production scheduling, where solution time directly impacts operational feasibility, and MIP-based alternatives would be prohibitively expensive.

An important limitation of our approach is its convexity requirement. As such, our method complements Neur2SP by excelling in convex or convexifiable settings, whereas ReLU-based MIP formulations remain the most suitable choice for non-convex recourse. On the other hand, while our experiments focus on linear and mixed-integer recourse, the theoretical underpinnings of ICNNs suggest broader applicability to nonlinear convex settings, a promising direction for future work.

Additionally, the field of 2SP suffers from a scarcity of standardised, challenging benchmarks. Existing instances often lack the scale and complexity of modern industrial problems. Validating ICNN-enhanced 2SP on emerging applications will be critical to assessing its practical value. Finally, the interplay between ICNNs and problem structure, particularly in partially convex regimes, warrants deeper exploration, as hybrid architectures could unlock solutions to previously intractable stochastic programs. By bridging convex optimisation and deep learning, this work takes important steps further for scalable, trustworthy decision-making under uncertainty.

Acknowledgments and Disclosure of Funding

We acknowledge the computational resources provided by the Aalto Science-IT project. Yu Liu gratefully acknowledges the support from the China Scholarship Council and thanks Yuanxiang Yang for insightful discussions.

References

- Agrawal, S., Jia, R., 2019. Learning in Structured MDPs with Convex Cost Functions: Improved Regret Bounds for Inventory Management, in: Proceedings of the 2019 ACM Conference on Economics and Computation, Association for Computing Machinery, New York, NY, USA. pp. 743–744. doi:10.1145/3328526.3329565.
- Ahmed, S., Garcia, R., Kong, N., Ntamo, L., Perboli, G., Qiu, F., Sen, S., 2015. SIPLIB: A Stochastic Integer Programming Test Problem Library. URL: <https://www2.isye.gatech.edu/~sahmed/siplib/>.
- Amos, B., Xu, L., Kolter, J.Z., 2017. Input Convex Neural Networks, in: Proceedings of the 34th International Conference on Machine Learning, PMLR. pp. 146–155. URL: <https://proceedings.mlr.press/v70/amos17b.html>.
- Birge, J.R., Louveaux, F., 2011. Introduction to Stochastic Programming. Springer Series in Operations Research and Financial Engineering, Springer, New York, NY. doi:10.1007/978-1-4614-0237-4.
- Boyd, S.P., Vandenberghe, L., 2004. Convex optimization. Cambridge university press. doi:10.1017/CB09780511804441.
- Bünning, F., Schalbetter, A., Aboudonia, A., Badyn, M.H.d., Heer, P., Lygeros, J., 2021. Input Convex Neural Networks for Building MPC, in: Proceedings of the 3rd Conference on Learning for Dynamics and Control, PMLR. pp. 251–262. URL: <https://proceedings.mlr.press/v144/bunning21a.html>.
- Carøe, C.C., Schultz, R., 1999. Dual decomposition in stochastic integer programming. Operations Research Letters 24, 37–45. doi:10.1016/S0167-6377(98)00050-9.
- Chen, Y., Shi, Y., Zhang, B., 2020. Data-Driven Optimal Voltage Regulation Using Input Convex Neural Networks. Electric Power Systems Research 189, 106741. doi:10.1016/j.epsr.2020.106741.
- Cornuejols, G., Sridharan, R., Thizy, J.M., 1991. A comparison of heuristics and relaxations for the capacitated plant location problem. European Journal of Operational Research 50, 280–297. doi:10.1016/0377-2217(91)90261-S.
- Dai, H., Xue, Y., Syed, Z., Schuurmans, D., Dai, B., 2021. Neural Stochastic Dual Dynamic Programming. doi:10.48550/arXiv.2112.00874.
- Duchesne, L., Louveaux, Q., Wehenkel, L., 2021. Supervised learning of convex piecewise linear approximations of optimization problems, in: Proceedings of the 29th European Symposium on Artificial Neural Networks, Computational Intelligence and Machine Learning (ESANN), pp. 493–498. doi:10.14428/esann/2021.ES2021-74.
- Dumouchelle, J., Patel, R., Khalil, E.B., Bodur, M., 2022. Neur2SP: Neural Two-Stage Stochastic Programming. doi:10.48550/arXiv.2205.12006.
- Fischetti, M., Jo, J., 2018. Deep neural networks and mixed integer linear optimization. Constraints 23, 296–309. doi:10.1007/s10601-018-9285-6.
- Gurobi Optimization, LLC, 2024. Gurobi Optimizer Reference Manual. URL: <https://www.gurobi.com>.
- Gurobi Optimization, LLC, 2025. Parameter Reference - Gurobi Optimizer Reference Manual. URL: <https://docs.gurobi.com/projects/optimizer/en/current/reference/parameters.html>.
- Heitsch, H., Römisich, W., 2003. Scenario Reduction Algorithms in Stochastic Programming. Computational Optimization and Applications 24, 187–206. doi:10.1023/A:1021805924152.
- Jiang, K., Hu, C., Yan, F., 2022. Path-following control of autonomous ground vehicles based on input convex neural networks. Proceedings of the Institution of Mechanical Engineers, Part D: Journal of Automobile Engineering 236, 2806–2816. doi:10.1177/09544070221114690.

- Khor, C.S., Elkamel, A., Ponnambalam, K., Douglas, P.L., 2008. Two-stage stochastic programming with fixed recourse via scenario planning with economic and operational risk management for petroleum refinery planning under uncertainty. *Chemical Engineering and Processing: Process Intensification* 47, 1744–1764. doi:10.1016/j.cep.2007.09.016.
- Küçükyavuz, S., Sen, S., 2017. An Introduction to Two-Stage Stochastic Mixed-Integer Programming, in: *Leading Developments from INFORMS Communities*. INFORMS. INFORMS TutORials in Operations Research, pp. 1–27. doi:10.1287/educ.2017.0171.
- Larsen, E., Frejinger, E., Gendron, B., Lodi, A., 2024. Fast Continuous and Integer L-Shaped Heuristics Through Supervised Learning. *INFORMS Journal on Computing* 36, 203–223. doi:10.1287/ijoc.2022.0175.
- Luxenberg, E., Boyd, S., 2024. Portfolio construction with Gaussian mixture returns and exponential utility via convex optimization. *Optimization and Engineering* 25, 555–574. doi:10.1007/s11081-023-09814-y.
- Ntaimo, L., Sen, S., 2005. The Million-Variable “March” for Stochastic Combinatorial Optimization. *Journal of Global Optimization* 32, 385–400. doi:10.1007/s10898-004-5910-6.
- Omidi, A., Mishra, T., Almassalkhi, M.R., 2024. Towards Input-Convex Neural Network Modeling for Battery Optimization in Power Systems. doi:10.48550/arXiv.2410.09166.
- Paszke, A., Gross, S., Massa, F., Lerer, A., Bradbury, J., Chanan, G., Killeen, T., Lin, Z., Gimelshein, N., Antiga, L., Desmaison, A., Kopf, A., Yang, E., DeVito, Z., Raison, M., Tejani, A., Chilamkurthy, S., Steiner, B., Fang, L., Bai, J., Chintala, S., 2019. PyTorch: An imperative style, high-performance deep learning library, in: Wallach, H., Larochelle, H., Beygelzimer, A., d'Alché-Buc, F., Fox, E., Garnett, R. (Eds.), *Advances in Neural Information Processing Systems* 32. Curran Associates, Inc., pp. 8024–8035. URL: <https://dl.acm.org/doi/10.5555/3454287.3455008>.
- Patel, R., Dumouchelle, J., 2022. Khalil-research/Neur2SP. URL: <https://github.com/khalil-research/Neur2SP>.
- Pedregosa, F., Varoquaux, G., Gramfort, A., Michel, V., Thirion, B., Grisel, O., Blondel, M., Prettenhofer, P., Weiss, R., Dubourg, V., Vanderplas, J., Passos, A., Cournapeau, D., Brucher, M., Perrot, M., Édouard Duchesnay, 2011. Scikit-learn: Machine learning in python. *Journal of Machine Learning Research* 12, 2825–2830. URL: <http://jmlr.org/papers/v12/pedregosa11a.html>.
- Rosemberg, A., Tanneau, M., Fanzeres, B., Garcia, J., Van Hentenryck, P., 2024. Learning Optimal Power Flow value functions with input-convex neural networks. *Electric Power Systems Research* 235, 110643. doi:10.1016/j.epsr.2024.110643.
- Römisch, W., Vigerske, S., 2010. Recent Progress in Two-stage Mixed-integer Stochastic Programming with Applications to Power Production Planning, in: Pardalos, P.M., Rebennack, S., Pereira, M.V.F., Iliadis, N.A. (Eds.), *Handbook of Power Systems I*. Springer, Berlin, Heidelberg, pp. 177–208. doi:10.1007/978-3-642-02493-1_8.
- Schultz, R., Stougie, L., van der Vlerk, M.H., 1998. Solving stochastic programs with integer recourse by enumeration: A framework using Gröbner basis. *Mathematical Programming* 83, 229–252. doi:10.1007/BF02680560.
- Shapiro, A., Homem-de Mello, T., 1998. A simulation-based approach to two-stage stochastic programming with recourse. *Mathematical Programming* 81, 301–325. doi:10.1007/BF01580086.
- Sherali, H.D., Fraticelli, B.M., 2002. A modification of Benders’ decomposition algorithm for discrete subproblems: An approach for stochastic programs with integer recourse. *Journal of Global Optimization* 22, 319–342. doi:10.1023/A:1013827731218.
- Varga, J., Karlsson, E., Raidl, G.R., Rönnberg, E., Lindsten, F., Rodemann, T., 2024. Speeding Up Logic-Based Benders Decomposition by Strengthening Cuts with Graph Neural Networks, in: Nicosia, G., Ojha, V., La Malfa, E., La Malfa, G., Pardalos, P.M., Umeton, R. (Eds.), *Machine Learning, Optimization, and Data Science*, Springer Nature Switzerland, Cham. pp. 24–38. doi:10.1007/978-3-031-53969-5_3.

- Wang, W., Zhang, H., Wang, Y., Tian, Y., Wu, Z., 2024. Fast Explicit Machine Learning-Based Model Predictive Control of Nonlinear Processes Using Input Convex Neural Networks. *Industrial & Engineering Chemistry Research* 63, 17279–17293. doi:10.1021/acs.iecr.4c02257.
- Yang, S., Bequette, B.W., 2021. Optimization-based control using input convex neural networks. *Computers & Chemical Engineering* 144, 107143. doi:10.1016/j.compchemeng.2020.107143.
- Yilmaz, D., Büyüktaktın, İ.E., 2024. A deep reinforcement learning framework for solving two-stage stochastic programs. *Optimization Letters* 18, 1993–2020. doi:10.1007/s11590-023-02009-5.
- Zhong, H., Yan, X., Tan, Z., 2021. Real-Time Distributed Economic Dispatch Adapted to General Convex Cost Functions: A Secant Approximation-Based Method. *IEEE Transactions on Smart Grid* 12, 2089–2101. doi:10.1109/TSG.2020.3049054.

Technical Appendices and Supplementary Material

A MIP reformulations

This appendix details the MIP formulation required to embed conventional ReLU NNs into optimisation problems, highlighting the additional complexity that our ICNN-based approach avoids.

Consider a conventional ReLU NN with $L + 1$ layers (numbered from 0 to L) to build the surrogate model of an underlying function f , which can be approximated and effectively replaced using this ReLU NN surrogate \hat{f} , constructed based on dataset \mathcal{D} . For the input layer, we have $y^0 = x$. For the output layer we have $y^L = \hat{f}_{\mathcal{D}}(x)$. The activation of neurons $i = 1, \dots, N_l$ in the hidden layer $l = 1, \dots, L - 1$ are calculated as

$$y_i^l = \text{ReLU}(w_i^{l\top} y_{l-1} + b_i^l) = \max(0, w_i^{l\top} y_{l-1} + b_i^l), \quad (16)$$

where w_i^l and b_i^l denote the weight and bias of the corresponding neuron, respectively. Suppose we could obtain the lower bounds $L_i^l < 0$ and upper bounds $U_i^l > 0$ such that

$$L_i^l \leq w_i^{l\top} y_{l-1} + b_i^l \leq U_i^l. \quad (17)$$

Following Fischetti and Jo (2018), the ReLU operator can be encoded into mixed-integer linear constraints by introducing slack variables s_i^l and binary variables z_i^l for $i = 1, \dots, N_l$, $l = 1, \dots, L - 1$, which is expressed as:

$$y_i^l - s_i^l = w_i^{l\top} y^{l-1} + b_i^l, \quad (18)$$

$$0 \leq y_i^l \leq U_i^l z_i^l, \quad (19)$$

$$0 \leq s_i^l \leq -L_i^l (1 - z_i^l), \quad (20)$$

$$z_i^l \in \{0, 1\}. \quad (21)$$

Combining these constraints with input and output layer bounds

$$L^0 \leq y^0 \leq U^0, \quad (22)$$

$$L^L \leq y^L = w^{L\top} y^{L-1} + b^L \leq U^L, \quad (23)$$

we obtain the exact MIP model to embed the ReLU NN surrogate $y = \hat{f}_{\mathcal{D}}(x)$ into a larger optimisation problem. This formulation necessarily introduces N binary variables, N continuous slack variables, and N activation value variables, where $N = \sum_{l=1}^{L-1} N_l$ represents the total number of neurons across all hidden layers. The inclusion of these binary variables fundamentally alters the computational complexity class of the resulting optimisation problem, leading to exponential worst-case solution time as network size increases.

B Stochastic programming problems

This appendix provides brief descriptions of the three benchmark problems employed in our experimental evaluation. These are the same problems utilised in Dumouchelle et al. (2022), facilitating direct comparison between our ICNN-enhanced approach and the Neur2SP methodology.

B.1 Capacitated facility location problem (CFLP)

The CFLP addresses the challenge of selecting optimal facility locations to service customer demand at minimal cost. In its stochastic formulation, facility decisions precede knowledge of actual demand patterns. Our implementation adapts the case from Cornuejols et al. (1991) to the stochastic setting by preserving the original cost structures and capacity parameters while stochastically sampling demand values. To guarantee relatively complete recourse, we incorporate penalty variables for potential demand shortfalls. Throughout our experimental analysis, we denote a CFLP instance with n facilities, m customers, and s scenarios as CFLP_ n _ m _ s .

Table 5: Data generation time (5,000 samples per instance) utilising 16 parallel processes.

Problem	(IC)NN	
	Time per sample (s)	Total time (s)
CFLP_10_10	0.32	1,620.07
CFLP_25_25	2.22	11,096.88
CFLP_50_50	2.19	10,945.11
SSLP_5_25	0.84	4,182.60
SSLP_15_45	2.49	12,438.02
SSLP_10_50	2.33	11,649.44
INVP_B_E	1.77	8,855.89
INVP_B_H	1.43	7,157.07
INVP_I_E	1.48	7,420.66
INVP_I_H	1.04	5,194.90

B.2 Stochastic server location problem (SSLP)

The SSLP focuses on optimal server deployment and client assignment under uncertain service requests. Binary first-stage variables determine server placement, while second-stage variables manage client-server assignments after observing which clients require service. Our experimental protocol utilises the standard benchmark instances from SIPLIB Ahmed et al. (2015) as documented in Ntaimo and Sen (2005). For consistent reference, we denote an SSLP instance with n potential server locations, m possible clients, and s scenarios as $\text{SSLP}_{n,m,s}$.

B.3 Investment problem (INVP)

The INVP consists of continuous first-stage investment decisions followed by discrete second-stage profit-generating activities. We implement Example 7.3 from Schultz et al. (1998), with two first-stage variables bounded by $[0, 5]$ and four binary second-stage variables. Scenarios derive from two random variables uniformly distributed over $[5, 15]$. For consistency, we reformulate it as a minimisation problem. In our experiments, we denote instances as $\text{INVP}_{v,t,s}$, where v indicates second-stage variable type (B for binary, I for integer), t indicates technology matrix type (E for identity, H for $[[2/3, 1/3], [1/3, 2/3]]$), and s indicates the number of scenarios.

C Data generation

Table 5 reports computational time for generating the shared 5,000-sample dataset used to train both NN and ICNN surrogates for the expected recourse function. Under the dataset generation setting as described in Section 5.1, for each of the 5,000 first-stage solutions, we randomly sample between 1 and 100 scenarios (averaging ~ 50 scenarios per solution), resulting in approximately $5,000 \times 50 = 250,000$ second-stage optimisation problems to solve for each problem instance. Notably, this process is highly parallelisable and could be extended to utilise more computational resources when available.

D Model selection

For model selection, we conducted a random search over 100 configurations for each problem instance following Dumouchelle et al. (2022). Both the ICNN-enhanced 2SP and Neur2SP methods were subjected to identical hyperparameter sampling from the distribution space outlined in Table 6, with training proceeding for 2,000 epochs across all configurations.

To ensure fair comparison, we constrained the architecture of both methods to utilise a single ReLU hidden layer with varying dimensionality within Φ . For the Scenario Encoding component, which precedes surrogate training as described in Section 4.1, we implemented a three-layer architecture. Specifically, “Embed hidden dimension 1” and “Embed hidden dimension 2” correspond to the layers before scenario aggregation (within Ψ^1), while “Embed hidden dimension 3” represents the final

Table 6: NN hyperparameter sampling space. Values in $\{\}$: equal probability sampling; values in $[\]$: uniform distribution sampling.

Parameter	Sampling range
Batch size	$\{16, 32, 64, 128\}$
Learning rate	$[1e^{-5}, 1e^{-1}]$
L1 weight penalty	$[1e^{-5}, 1e^{-1}]$
L2 weight penalty	$[1e^{-5}, 1e^{-1}]$
Optimiser	$\{\text{Adam, Adagrad, RMSprop}\}$
Dropout	$[0, 0.5]$
ReLU hidden dimension	$\{64, 128, 256, 512\}$
Embed hidden dimension 1	$\{64, 128, 256, 512\}$
Embed hidden dimension 2	$\{16, 32, 64, 128\}$
Embed hidden dimension 3	$\{8, 16, 32, 64\}$

Table 7: Solver parameter settings in the experiments.

Parameter	Value	Description
TimeLimit	10800	Limit total runtime (3 h)
Threads	1	Thread count
Presolve	0	Disable presolve
Heuristics	0	Minimise time spent in MIP heuristics
NodeMethod	1	Use dual simplex for MIP node relaxations
Cuts	1	Moderate cut generation
MIPFocus	2	Focus on proving optimality

hidden layer after aggregation (within Ψ^2). This configuration allows the model to effectively distil scenario information into the fixed vector representation ξ_λ .

E Solver parameter settings

Gurobi’s automatic parameter selection introduces variability in results due to divergent solution strategies rather than formulation differences. To isolate methodological comparisons, we fix key Gurobi parameters (Table 7), standardising the solving environment across formulations. See Gurobi Optimization, LLC (2025) for details.

F Objective results

This section presents a detailed comparison of objective function values obtained through different solution approaches. We report the objective values of the EF formulation as the baseline, which represents the best solutions found within the time limit. Additionally, we report two sets of objectives for solutions obtained via surrogate embedding reformulations: the “true objective” and the “approximate objective”. Tables 8 through 10 present these comparative values. The results demonstrate that the ICNN-enhanced approach consistently achieves solution quality on par with or better than conventional NN approaches while maintaining computational advantages discussed in the main paper.

G SSLP SIPLIB results

This section presents performance metrics for the SSLP instances from SIPLIB (Ahmed et al., 2015). Table 11 reports optimality gaps and solving times across different problem configurations.

The results reveal that ICNN-enhanced 2SP achieves optimal or near-optimal solutions (0-1.63% gaps) across all instances. For medium-sized SSLP_15_45 instances, ICNN-enhanced 2SP significantly outperforms Neur2SP in solution quality while maintaining comparable solving times. This notable performance divergence suggests that the ICNN architecture better captures the underlying structure

Table 8: Objectives for CFLP (averaged over 11 instances per row). Baseline: EF objective at termination. True objective: cost of first-stage solutions from surrogate methods evaluated on original scenarios. Approximate objective: direct values from surrogate reformulations. ICNN: ICNN-enhanced 2SP, NN: Neur2SP. **Bold** indicates better solutions.

Problem	Baseline	True objective		Approximate objective	
		ICNN	NN	ICNN	NN
CFLP_10_10_100	6,994.77	7,034.16	7,030.35	7,172.48	7,155.62
CFLP_10_10_500	7,003.30	7,013.85	7,003.30	7,179.69	7,151.01
CFLP_10_10_1000	7,013.16	7,011.28	6,994.31	7,158.10	7,135.23
CFLP_25_25_100	11,854.23	12,109.66	12,252.05	12,760.21	11,396.54
CFLP_25_25_500	11,856.48	12,109.66	12,160.15	12,760.21	11,396.54
CFLP_25_25_1000	11,997.73	12,109.66	12,162.84	12,760.21	11,396.54
CFLP_50_50_100	25,573.72	26,418.27	30,205.61	26,122.57	23,556.44
CFLP_50_50_500	29,352.39	26,379.70	30,172.44	26,122.57	23,556.44
CFLP_50_50_1000	30,278.57	26,395.75	30,194.65	26,122.57	23,556.44

Table 9: Objectives for SSLP (averaged over 12 instances per row). Same column definitions as in Table 8.

Problem	Baseline	True objective		Approximate objective	
		ICNN	NN	ICNN	NN
SSLP_5_25_50	-125.36	-125.22	-125.22	-119.09	-124.47
SSLP_5_25_100	-120.94	-120.91	-120.91	-119.09	-124.47
SSLP_15_45_5	-255.55	-248.44	-208.49	-243.23	-227.99
SSLP_15_45_10	-257.41	-250.62	-209.98	-248.01	-227.99
SSLP_15_45_15	-257.69	-252.17	-209.08	-248.01	-237.45
SSLP_10_50_50	-354.96	-354.96	-354.96	-357.70	-355.18
SSLP_10_50_100	-345.86	-345.86	-345.86	-357.70	-355.18
SSLP_10_50_500	-349.54	-349.54	-349.54	-357.70	-355.18
SSLP_10_50_1000	-342.64	-350.07	-350.07	-357.70	-355.18
SSLP_10_50_2000	-172.74	-350.07	-350.07	-357.70	-355.18

of these specific problem instances. Computational efficiency advantages of ICNN-enhanced 2SP increase with problem complexity. For smaller instances (SSLP_5_25), ICNN shows approximately 2× speedup over Neur2SP. For the largest instances (SSLP_10_50), both surrogate methods vastly outperform EF, while ICNN-enhanced 2SP consistently requires approximately one-third the solving time of Neur2SP for these challenging instances.

H Formulation size

We compare variable counts of the surrogate embedding reformulation between ICNN-enhanced 2SP (our method) and Neur2SP (MIP-based method) in Table 12. As detailed in Section 4, ICNN’s convex structure avoids introducing new integer variables and halves the auxiliary continuous variables required by Neur2SP’s ReLU activation encodings.

For integer variables: ICNN uses only original first-stage integers (e.g., in CFLP/SSLP; none in INVP); Neur2SP adds auxiliary integers to encode ReLU activations. For continuous variables: ICNN requires 50% fewer auxiliary variables than Neur2SP with equivalent network architectures. This reduction stems from ICNN’s LP-representable structure that requires only one additional variable per neuron, whereas ReLU networks in Neur2SP require two (one for the activation output and one slack variable). Network architecture impacts reformulation complexity. *Italic* entries mark instances where both methods share identical architectures (same hidden layer dimension) after hyperparameter tuning. In these cases, ICNN’s reformulation efficiency is most pronounced, with variable count reductions directly attributable to methodological differences rather than model size variations.

Table 10: Objectives for INVP (one instance per row). Same column definitions as in Table 8.

Problem	Baseline	True objective		Approximate objective	
		ICNN	NN	ICNN	NN
ip_B_E_4	-57.00	-50.70	-50.84	-59.15	-58.58
ip_B_E_9	-59.33	-56.01	-56.78	-59.63	-59.27
ip_B_E_36	-61.22	-59.21	-58.42	-59.69	-59.30
ip_B_E_121	-62.29	-60.38	-60.51	-59.62	-59.62
ip_B_E_441	-61.32	-59.42	-59.37	-59.56	-59.70
ip_B_E_1681	-60.52	-59.93	-60.39	-59.57	-60.00
ip_B_E_10000	-59.09	-60.02	-60.06	-60.27	-60.03
ip_B_H_4	-56.75	-51.75	-51.75	-55.70	-59.17
ip_B_H_9	-59.56	-56.56	-56.56	-57.22	-59.11
ip_B_H_36	-60.28	-59.31	-59.31	-59.38	-59.58
ip_B_H_121	-61.01	-59.93	-59.93	-59.72	-59.96
ip_B_H_441	-61.44	-60.14	-60.14	-60.50	-60.07
ip_B_H_1681	-60.89	-60.47	-60.47	-61.52	-60.09
ip_B_H_10000	-58.93	-60.53	-60.53	-61.07	-60.29
ip_I_E_4	-63.50	-60.47	-52.50	-65.31	-76.35
ip_I_E_9	-66.56	-65.84	-61.89	-66.19	-76.46
ip_I_E_36	-69.86	-69.60	-67.08	-66.79	-71.99
ip_I_E_121	-71.12	-70.99	-69.07	-67.24	-75.88
ip_I_E_441	-69.64	-69.56	-67.39	-67.34	-75.71
ip_I_E_1681	-68.85	-68.56	-66.52	-67.48	-75.82
ip_I_E_10000	-68.05	-67.90	-65.67	-67.57	-75.79
ip_I_H_4	-63.50	-54.75	-54.75	-65.10	-65.33
ip_I_H_9	-65.78	-61.93	-59.78	-63.71	-65.48
ip_I_H_36	-67.11	-64.63	-63.78	-65.57	-66.44
ip_I_H_121	-67.75	-65.21	-65.03	-66.99	-66.76
ip_I_H_441	-67.24	-66.38	-65.12	-66.99	-66.76
ip_I_H_1681	-65.41	-65.68	-65.63	-66.99	-66.73
ip_I_H_10000	-65.82	-65.65	-65.66	-66.98	-67.01

Table 11: Performance comparison for SSLP SIPLIB instances. ICNN: ICNN-enhanced 2SP, NN: Neur2SP, EF: Extensive Form (baseline). **Bold** indicates superior performance between ICNN and NN (lower is better). Optimal reference values from Ahmed et al. (2015).

Problem	Gap to optimum (%)			Solving time (s)		
	ICNN	NN	EF	ICNN	NN	EF
SSLP_5_25_50	0.00	0.00	0.00	0.12	0.24	1.46
SSLP_5_25_100	0.00	0.00	0.00	0.12	0.26	5.44
SSLP_15_45_5	0.53	18.90	0.00	0.16	0.19	3.36
SSLP_15_45_10	1.54	18.23	0.00	0.16	0.20	1.57
SSLP_15_45_15	1.63	16.51	0.00	0.28	0.20	7.14
SSLP_10_50_50	0.00	0.00	0.00	0.27	0.77	10,800.02
SSLP_10_50_100	0.00	0.00	0.00	0.26	0.76	10,800.16
SSLP_10_50_500	0.00	0.00	0.00	0.24	0.76	10,800.59
SSLP_10_50_1000	0.00	0.00	4.77	0.27	0.75	10,800.08
SSLP_10_50_2000	0.00	0.00	51.24	0.27	0.76	10,800.10

Table 12: Variable counts comparison between ICNN-enhanced 2SP and Neur2SP reformulations. *Italic* entries indicate instances with architecture parity after hyperparameter tuning.

Problem	# Continuous		# Integer (Binary)	
	ICNN	NN	ICNN	NN
<i>CFLP_10_10</i>	513	1025	10	522
<i>CFLP_25_25</i>	513	1025	25	537
<i>CFLP_50_50</i>	513	1025	50	562
<i>SSLP_5_25</i>	513	1025	5	517
<i>SSLP_15_45</i>	257	257	15	143
<i>SSLP_10_50</i>	513	1025	10	522
INVP_B_E	259	259	0	128
INVP_B_H	259	259	0	128
INVP_I_E	259	259	0	128
INVP_I_H	259	259	0	128